Supplement of Clim. Past, 15, 1537–1556, 2019
https://doi.org/10.5194/cp-15-1537-2019-supplement

Climate of the Past
Open Access

Supplement of

Spatial pattern of accumulation at Taylor Dome during Marine Isotope Stage 4: stratigraphic constraints from Taylor Glacier

James A. Menking et al.

Correspondence to: James A. Menking (james.menking@oregonstate.edu)

1 Tie Point Selections

1.1 Taylor Glacier MIS 5/4 cores

1.1.1 Gas age scale

Tie points matching features in CH_4 and $\delta^{18}O_{atm}$ to previous ice core records were chosen to generate the gas age scale for the new MIS 5/4 cores (Figure S1). The CH_4 tie points were chosen using both laboratory and field continuous datasets, which generally agree with each other below 4 m depth. Above 4 m the CH_4 data in some cases diverge substantially, likely due to contamination from resealed thermal cracks near the surface.

In the 0-4 m section two tie points were chosen from the continuous field CH_4 (purple line in Figure S1) because these data appear to capture the correct magnitude of changes in CH_4 associated with DO 16/17 despite the possibility of contamination. Given concerns about contamination in the upper four meters we assigned larger errors to those tie points. We did not match the discrete data from the field (brown markers in Figure S1) because they are lower quality (lower instrument precision and lower sampling resolution). The purpose of the discrete field data was for ice reconnaissance and to inform our core retrieval strategy. As discussed in the main text, we do not rely on gas data from 0-4 m for our conclusions and include them here only for completeness.

Additional methane tie points match the midpoint of the DO 16/17 CH_4 rise (4.19 m, 59.66 ka) and the low CH_4 value before the DO 16/17 rise (5.4 m, 59.94 ka). These ties are the most robust of the entire set because (1) the magnitude of the change in CH_4 makes the features unambiguous, and (2) the features are resolved in the continuous CH_4 data sets and the discrete measurements. A further CH_4 tie point at DO 18 (7.79, 64.90 ka) is robust because both continuous and discrete measurements captured variability in CH_4 there (Figure S1). Offsets between laboratory and field continuous CH_4 between 7.4-8 m are likely due to depth offsets (~ 20 cm depth uncertainty, described in the main text). The section of the core from 5-8 m is also where delta age (Δage) is the highest, implying the lowest accumulation (see main text). Thus it is possible that the offsets in CH_4 at ~ 8 m are also partially due to small-scale heterogeneities in firn smoothing that might have arisen as accumulation rates decreased to very low values.

Four final CH_4 tie points match variations associated with DO 19 (13.25 m, 71.21 ka and 16.20 m, 72.27 ka), and variations that occur just after DO 19 (11.24 m, 69.92 ka and 12.43 m, 70.62 ka). These tie points are robust given that the CH_4 variations are resolved by all four of our CH_4 datasets (laboratory and field continuous and discrete measurements) (Figure S1), and because the features are clearly resolved in the EDML CH_4 record.

$\delta^{18}O_{atm}$ tie points were picked to match the mid point of the transition between 74-72 ka in NGRIP and the first low value at the beginning of the transition. NGRIP $\delta^{18}O_{atm}$ data were used because they are the highest resolution and precision data we are aware of available on AICC 2012 (Figure S1). Siple Dome is not synchronized to AICC 2012 in this age range (Seltzer et al., 2017). Vostok data are much lower resolution, and TALDICE $\delta^{18}O_{atm}$ from the deeper core sections are unpublished. EDML data show reasonable agreement with NGRIP and are included in Figure 2 in the main text and Figure S1.

The oldest $\delta^{18}O_{atm}$ tie point, linking 19.27 m to 73.74 ka, is assigned large uncertainty in the older direction (74.5-73.35 ka) since the NGRIP $\delta^{18}O_{atm}$ record is relatively unchanging between 76-74 ka. The $\delta^{18}O_{atm}$ offset at ~ 17 m (Figure S1) is due to a depth offset between the MIS 5/4 core retrieved in 2014-2015 and the deeper section retrieved in 2015-2016. If the deeper data were shifted 20 cm deeper (which is our estimated depth uncertainty), the result would be a plausible monotonic trend in $\delta^{18}O_{atm}$. Unfortunately we have no way of knowing the exact magnitude of the depth offset because we lack overlapping data, so we have left the depth registry unchanged. The offset does not significantly affect our age model or our interpretations of Δage.

The close match between our new CH_4 data and the radiometrically dated $\delta^{18}O$-$CaCO_3$ record from Hulu Cave speleothems supports our gas age tie point choices (Figure S5).

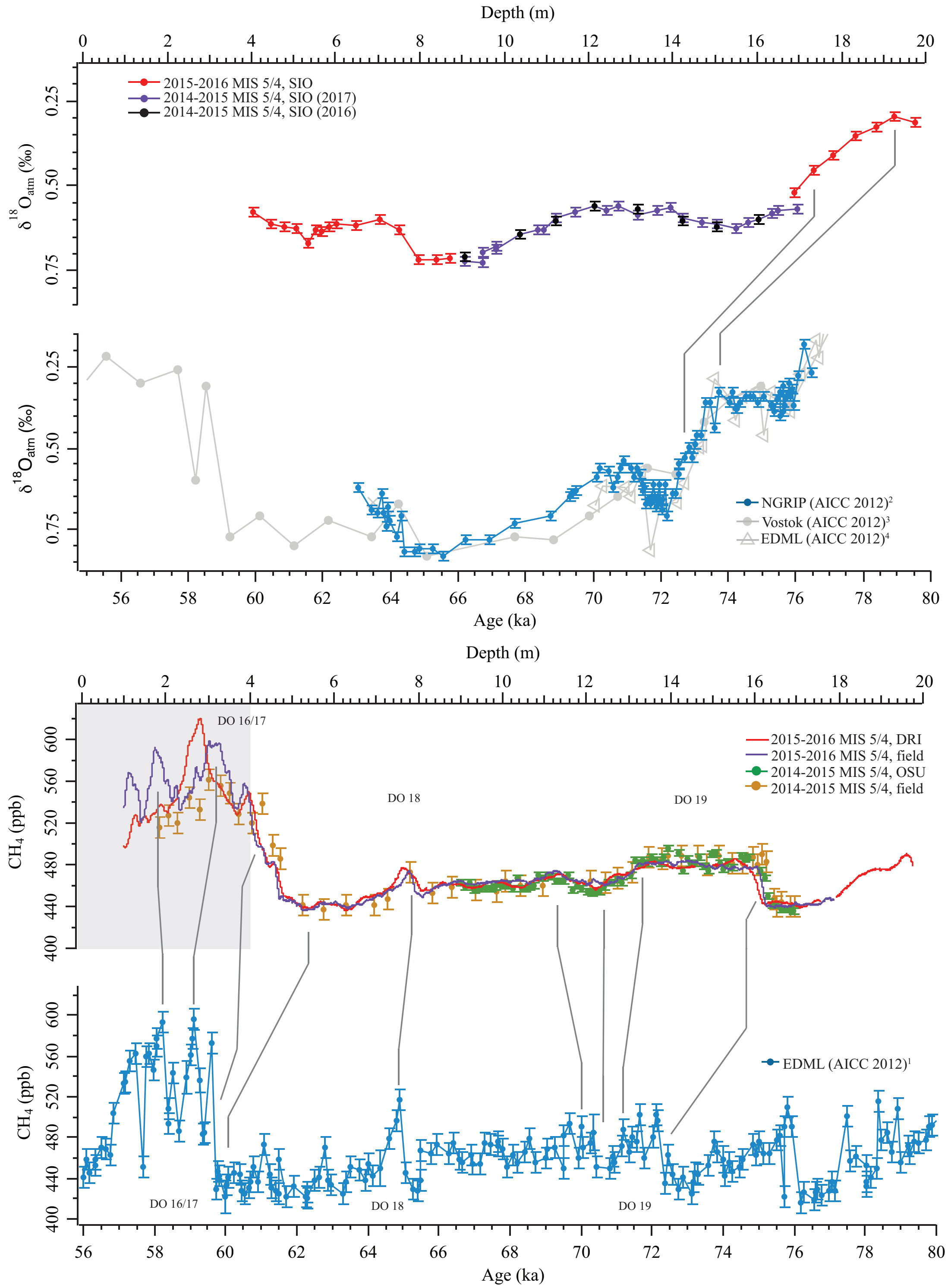

Figure S1 – Variability in new CH_4 and $\delta^{18}O_{atm}$ data from Taylor Glacier (on depth) and corresponding variability in ice cores on AICC 2012 (on age). $\delta^{18}O_{atm}$ data in black were measured in 2016, and data in purple were measured in 2017 including replication of some of the original measurements. Gray lines show the tie points described in the main text (Table 2). Gray shading indicates the section 0-4 m where gas data are potentially contaminated due to resealed surface cracks. CH_4 variability associated with particular Dansgaard Oeschger (DO) events are labeled by event number. Data references are denoted with superscripts: [1](Schilt et al., 2010), [2](Landais et al., 2007), [3](Petit et al., 1999), [4](Capron et al., 2010).

1.1.2 Ice age scale

Tie points matching features in Taylor Glacier MIS 5/4 non-sea salt Ca^{2+} ($nssCa^{2+}$), insoluble particle counts, and $\delta^{18}O_{ice}$ with features in EDC $nssCa^{2+}$, laser dust, and $\delta^{18}O_{ice}$ were chosen to generate the ice age scale for the new MIS 5/4 cores (Figure S2). The tie points were chosen using continuous datasets generated in the laboratory. Laboratory measurements of insoluble particle counts generally agree with field measurements, and small offsets in depth are due to the depth errors described in the main text (e.g., at ~ 9 m). Offsets in the magnitude of features resolved in the insoluble particle count records (e.g., the peak at ~ 1.2 m in the Taylor Glacier core) are due to the fact that the insoluble particle count data from the laboratory (red line in Figure S2) are 1 cm averages of the raw data, whereas the field data are not averaged (purple line in Figure S2). Taylor Glacier $nssCa^{2+}$ and insoluble particle count data are generally in good agreement (Figure S2 and Figure 2 in main text).

One place where the Taylor Glacier $nssCa^{2+}$ and insoluble particle counts are offset is in the top 40 cm of the MIS 5/4 ice core. For example the $nssCa^{2+}$ peak centered at 20 cm is offset from the insoluble particle peak centered at 34 cm (Figure S2). This is most apparent in Figure 2 in the main text (61.5-61 ka) where it appears that the peaks are more offset in age than most pairs of $nssCa^{2+}$-insoluble particle count peaks. This offset could be due to depth errors (up to 20 cm depth error), or it could be due to local deposition of non-Ca^{2+} dust into shallow cracks in the glacier surface that is known to affect ice shallower than 40 cm (Baggenstos et al., 2018). One tie point was chosen in ice shallower than 40 cm (0.34 m, 61.47 ka) because it appears to match a peak in the EDC laser dust record, though we assigned a large error range to the age to account for any ambiguity with the next oldest dust feature at 63.93 ka (total error range for this tie point = 63.93-59.5 ka). We do not interpret the data in the 0-40 cm section of the ice core except for presenting the one tie point as a plausible age. Excluding these data entirely would not change our conclusions, but we chose to display the data for completeness.

Eight more tie points match variability between EDC and Taylor Glacier MIS 5/4 dust data. Six of them match variability in $nssCa^{2+}$, and two match variability between Taylor Glacier insoluble particle counts and EDC laser dust. We opted for tie points using $nssCa^{2+}$ wherever possible given that $nssCa^{2+}$ is a more quantitative measurement than insoluble particle counts, and the $nssCa^{2+}$ record is generally less noisy than insoluble particle counts. Of the six $nssCa^{2+}$ tie points, the most robust are the tie points that match early features in the large dust increase that occurs at the MIS 4 onset (4-8 m depth, 72-68 ka). The dust fluctuations in this interval are unambiguous in the Taylor Glacier MIS 5/4 data as well as the EDC reference records (Figure S2). We tied two $nssCa^{2+}$ peaks (4.47 m, 68.63 ka and 5.60 m, 70.20 ka) and one $nssCa^{2+}$ low (4.94 m, 69.72 ka) to the variations in EDC $nssCa^{2+}$ in this interval.

Additional ice age tie points include $nssCa^{2+}$ tie points in MIS 4 (1.2 m, 63.93 ka and 3.10 m, 66.73 ka) (Figure 2 and Figure S2) and insoluble particle count tie points (1.80 m, 64.91 ka and 2.45 m, 65.65 ka) aligned with features in the EDC laser dust record. There may be ambiguity in some of these choices given the number of dust peaks in this interval. We stress that our manual choice of dust tie points in this section of the core qualitatively optimizes the match between the largest variations in both insoluble particle count and $nssCa^{2+}$ records – no peaks are skipped. We also note that the resulting depth-age curve (Figure 5a in main text) is relatively smooth.

Three tie points match variability in Taylor Glacier MIS 5/4 water isotopes to EDC water isotopes in the deeper part of the record (Figure S2). Although Taylor Glacier water isotopes are generally noisier than other Antarctic ice cores, we target unambiguously large changes in $\delta^{18}O_{ice}$ (2-3 ‰) and match them to features in EDC $\delta^{18}O_{ice}$ that are associated with AIM 19 and AIM 20. In order to identify the maximum and minimum values we smoothed the record and manually picked the highest and lowest values. The $\delta^{18}O_{ice}$ tie points are especially helpful given that dust variations are few and small in this section of the core.

A final $nssCa^{2+}$ tie point (19.76 m, 76.50 ka) is the least robust of the set given that there are no large features in $nssCa^{2+}$. We argue that the $nssCa^{2+}$ record at this tie point cannot be younger than the age uncertainty we assigned (77-75.75 ka), otherwise it would conflict with the preceding tie point at the AIM 20 $\delta^{18}O_{ice}$ maximum. The tie point cannot be older because we do not observe the small $nssCa^{2+}$ increase that occurs in EDC $nssCa^{2+}$ at 77 ka (Figure S2).

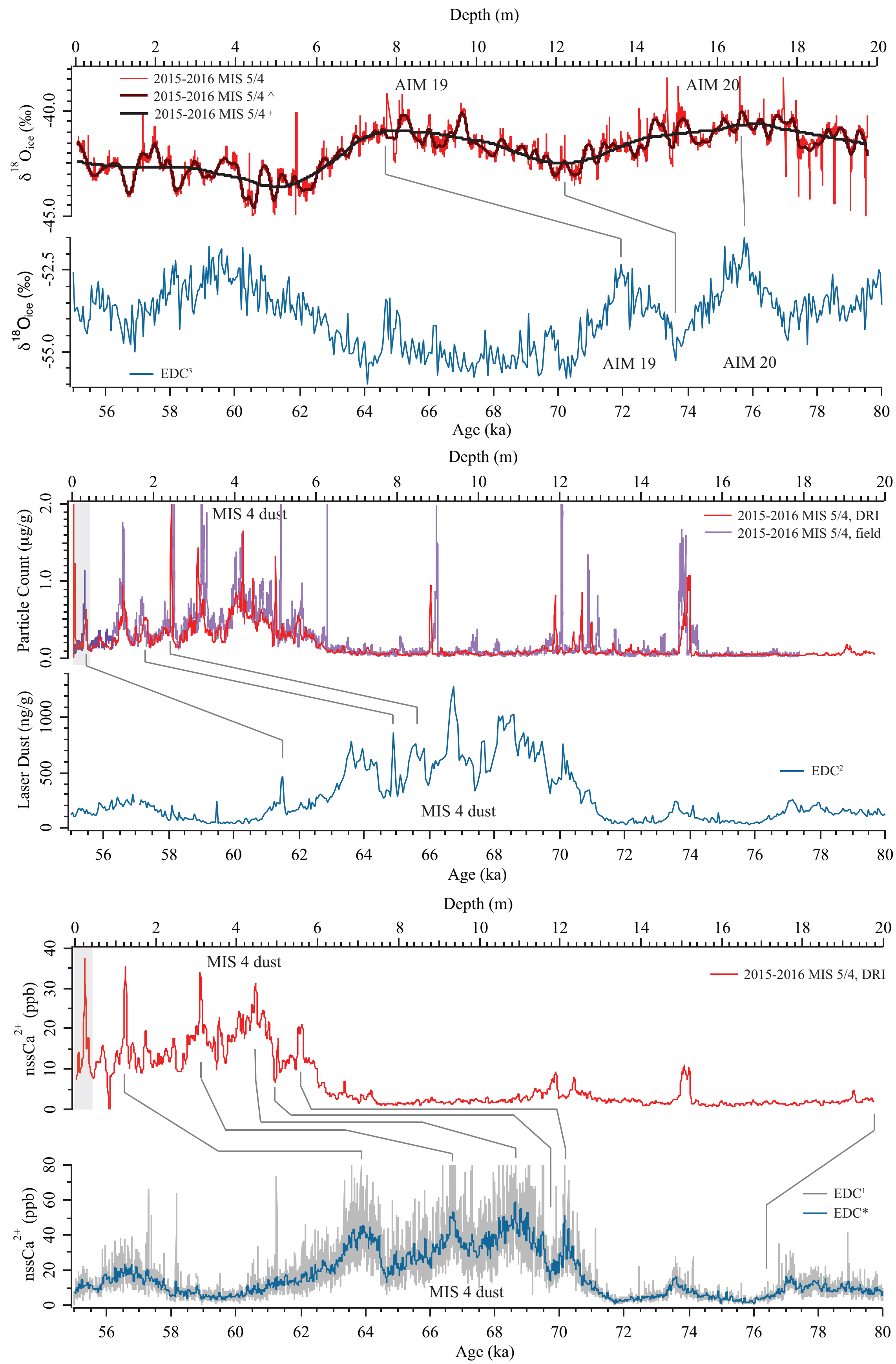

Depth (m)
2015-2016 MIS 5/4
2015-2016 MIS 5/4 ^
2015-2016 MIS 5/4 †
AIM 19
AIM 20
δ18Oice (‰)
EDC3
AIM 19
AIM 20
Age (ka)
Depth (m)
MIS 4 dust
2015-2016 MIS 5/4, DRI
2015-2016 MIS 5/4, field
Particle Count (µg/g)
Laser Dust (ng/g)
EDC2
MIS 4 dust
Age (ka)
Depth (m)
MIS 4 dust
2015-2016 MIS 5/4, DRI
nssCa2+ (ppb)
EDC1
EDC*
MIS 4 dust
Age (ka)

Figure S2 - Variability in new $nssCa^{2+}$, insoluble particle counts, and $\delta^{18}O_{ice}$ data from Taylor Glacier (on depth) and corresponding variability in ice cores synchronized to AICC 2012 (on age). Gray lines depict the tie points described in the main text (Table 3). Light gray shading indicates the top 0-40 cm where dust records may be contaminated by local dust deposition in surface cracks. Dust and water isotope variability associated with Marine Isotope Stage (MIS) 4 and Antarctic Isotope Maximum (AIM) events are labeled. *, ^, and † denote smoothing with 100 point, 500 point, and 5000 point LOESS algorithms, respectively. DRI particle count data are 1 cm averages. Data references are denoted with superscripts: [1] (Lambert et al., 2012), [2] (Lambert et al., 2008), [3] (Jouzel et al., 2007).

1.2 Taylor Dome

For the Taylor Dome ice core MIS 5/4 section many of the features we match are the same as the features discussed above.

1.2.1 Gas Age Scale

We adopted CO_2 tie points from Baggenstos et al. (2018) where our work overlaps (main text Figure 4). The remaining Taylor Dome gas age scale was constructed by matching features in CH_4 (Figure S3). Five tie points match features in new Taylor Dome CH_4 data to similar features in EDML CH_4. One tie point matches CH_4 variability at DO 21 (503.90 m, 83.90 ka), a feature older than the climate archive currently recovered from Taylor Glacier. One tie point is chosen from previously published CH_4 data (464.62 m, 59.99 ka) (Brook et al., 2000) to match the low CH_4 period immediately before the CH_4 rise associated with DO 16/17. The close match of the Taylor Dome CH_4 record on our revised age scale to the $\delta^{18}O$-$CaCO_3$ record from Hulu Cave speleothems supports our gas age tie point choices (Figure S5).

We adopted Ca^{2+} tie points from Baggenstos et al. (2018) where our work overlaps (Figure 4 in main text). Additionally we chose eight tie points to match variations in Taylor Dome Ca^{2+} (Mayewski et al., 1996) to variations in EDC $nssCa^{2+}$ and laser dust (Figure S4). Similar features are matched in the dusty MIS 4 section (482-461 m) as for the Taylor Glacier MIS 5/4 cores. The most robust tie points are at the onset of the high dust values (482-475 m, 72-68 ka). Two tie points matched variations in Taylor Dome Ca^{2+} to EDC laser dust data (463.30 m, 61.47 ka and 471.37 m, 65.57 ka) and helped optimize the fit such that no peaks were skipped.

Five $\delta^{18}O_{ice}$ tie points match variability in Taylor Dome $\delta^{18}O_{ice}$ to variations in EDC $\delta^{18}O_{ice}$ (Figure S4). Similar to the Taylor Glacier records, these tie points help construct the ice age model where there are small and few Ca^{2+} variations. One deep $\delta^{18}O_{ice}$ tie point is included (502.75 m, 83.9 ka) to complete the age scale back to the oldest CH_4 data (near DO 21).

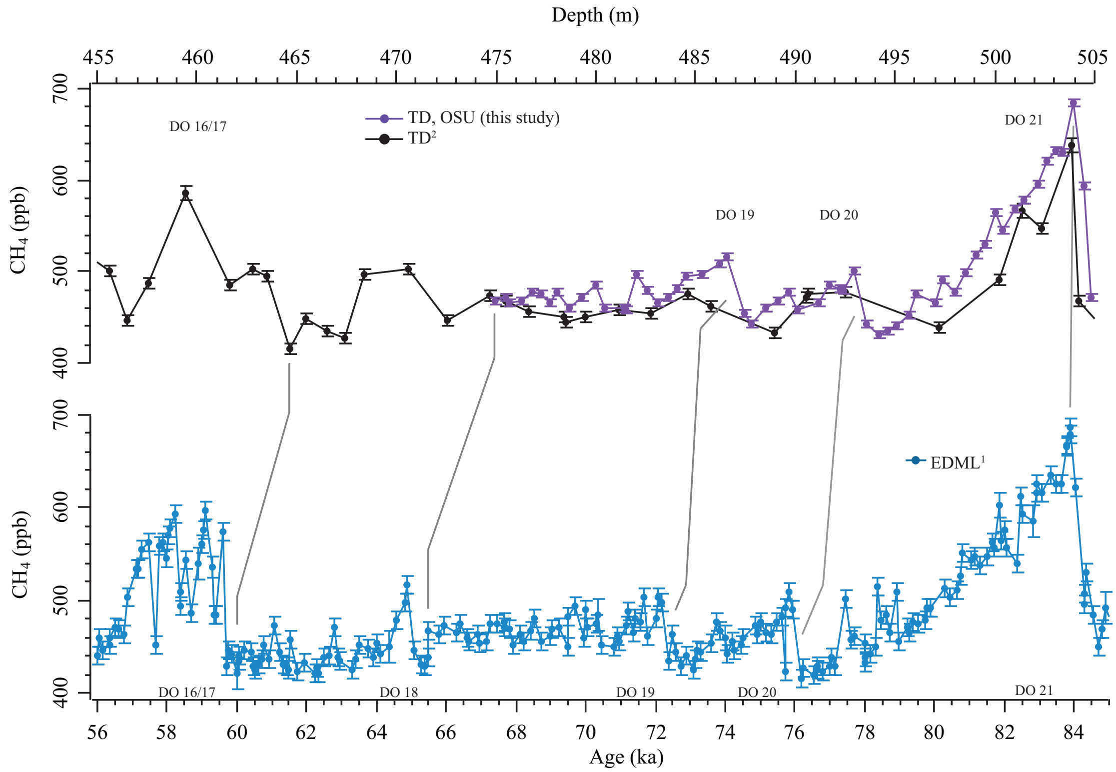

Figure S3 - Variability in new (purple) and previously published CH_4 data from Taylor Dome (on depth) and corresponding variability in the EPICA Dronning Maud Land (EDML) ice core synchronized to AICC 2012 (on age). Gray lines depict the tie points described in the main text (Table 5). CH_4 changes associated with particular Dansgaard-Oeschger (DO) events are labeled. Data references are denoted with superscripts: [1] (Schilt et al., 2010), [2] (Brook et al., 2000).

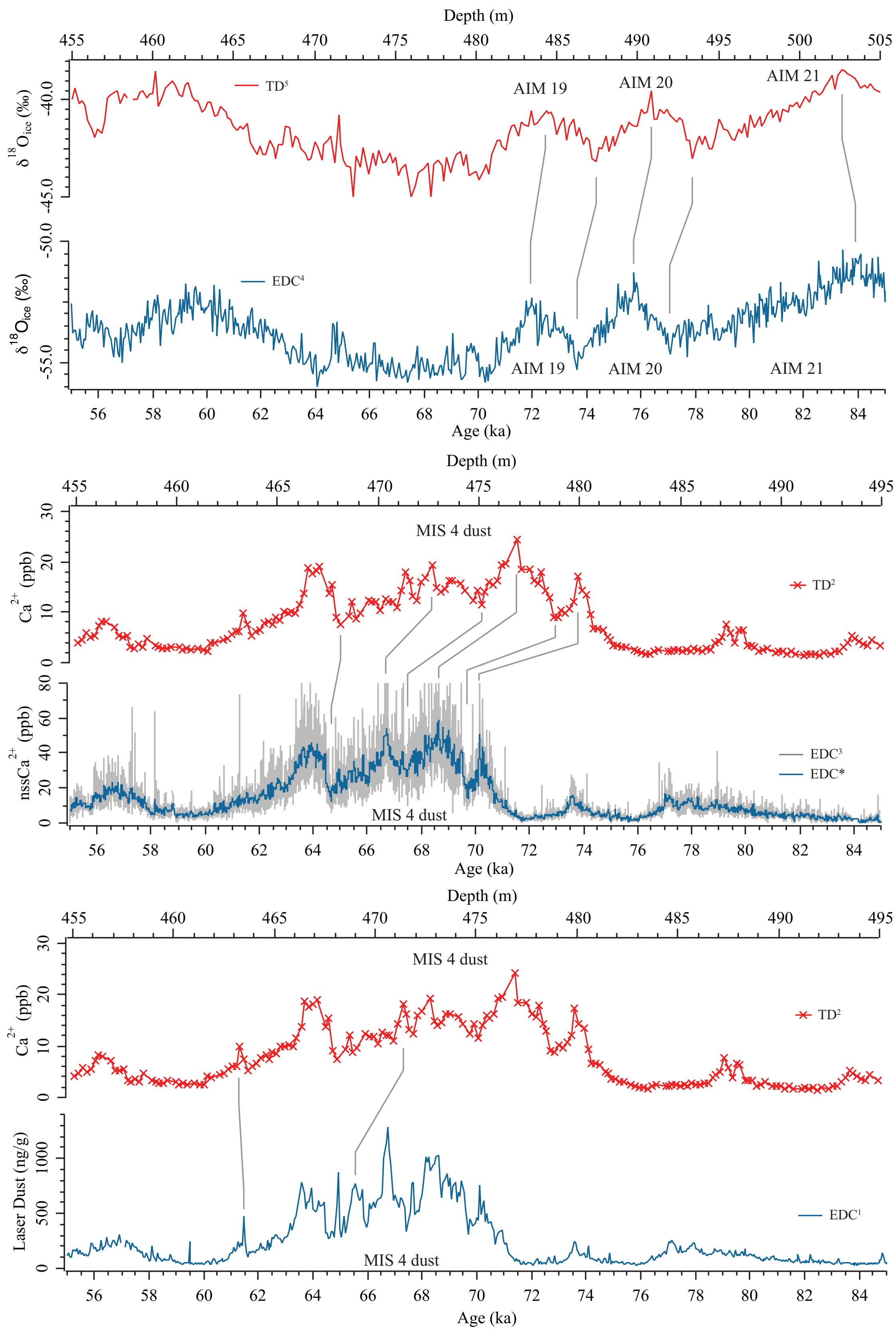
Depth (m)
455
460
465
470
475
480
485
490
495
500
505
δ18Oice (‰)
-40.0
-45.0
TD5
AIM 19
AIM 20
AIM 21
-50.0
-55.0
EDC4
56
58
60
62
64
66
68
70
72
74
76
78
80
82
84
Age (ka)
Ca2+ (ppb)
0
10
20
30
MIS 4 dust
TD2
nssCa2+ (ppb)
40
60
80
EDC3
EDC*
Laser Dust (ng/g)
500
1000
EDC1

Figure S4 - Variability in published Ca^{2+} and $\delta^{18}O_{ice}$ data from Taylor Dome (on depth) and corresponding variability in ice cores synchronized to AICC 2012 (on age). Gray lines depict the tie points described in the main text (Table 6). Dust and water isotope variations associated with MIS 4 and particular AIM events are labeled. * denotes smoothing with 100 point LOESS algorithm. Data references are denoted with superscripts: [1] (Lambert et al., 2008), [2] (Mayewski et al., 1996), [3] (Lambert et al., 2012), [4] (Jouzel et al., 2007), [5] (Steig et al., 1998).

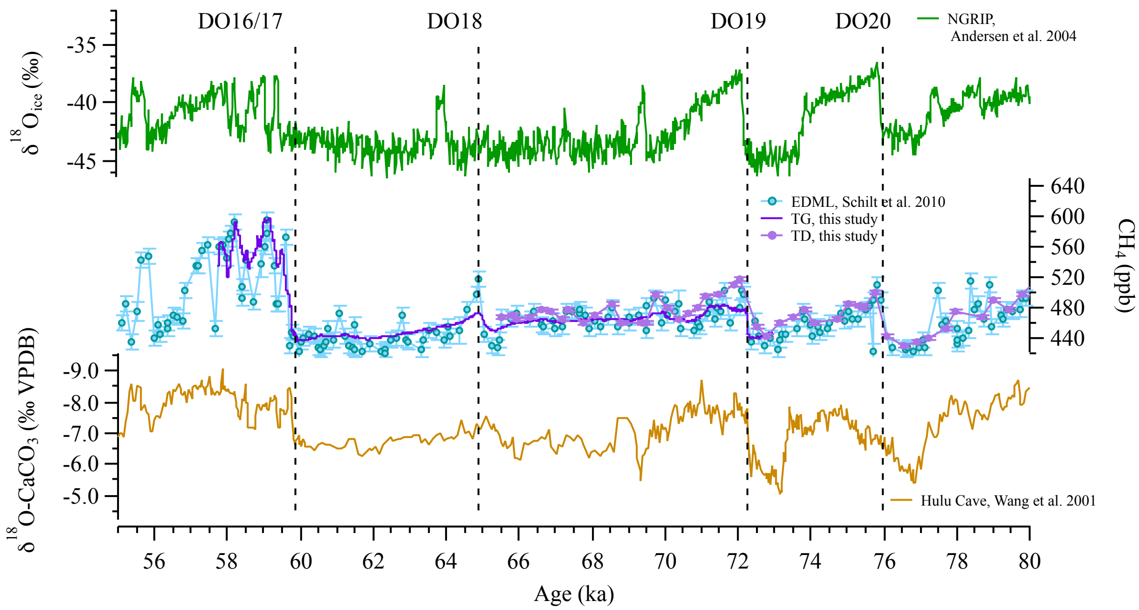

Figure S5 – Comparison of the timing of CH_4 changes in new Taylor Glacier and Taylor Dome data to the $\delta^{18}O$ measured in speleothems from Hulu Cave (Wang et al., 2001). Variations associated with particular DO events are labeled.

2 Firn modeling and accumulation rate estimate

We used the Herron and Langway (1980) firn densification model to calculate density-depth profiles for a range of temperatures (-50 to -40 ºC) and accumulation rates (0.0001-0.05 m yr^{-1} water equivalent) assuming surface snow density = 0.36 g cm^{-3}. The model calculates the first stage of densification to a threshold critical density = 0.55 g cm^{-3} with only site temperature as input (independent of accumulation rate). The second stage of densification (0.55 g cm^{-3} to bubble close-off) depends on temperature and accumulation rate. We assumed a density for bubble close-off of 0.83 g cm^{-3}. The close-off depth is the depth of the firn when it reaches the close-off density. We estimate Δage by calculating the age of the firn at the close-off depth using Herron and Langway's equation 11 (Figure S6). Accumulation can be estimated by looking up the accumulation rate that corresponds to a given temperature and Δage.

The height of the diffusive column of air in the firn is described by equation 1:

$$h_{diff} = d_{close-off} - h_{LIZ} - h_{conv} \qquad (1)$$

where $d_{close\text{-}off}$ is the close-off depth determined by the firn model, h_{LIZ} is the height of the lock-in zone where molecular diffusion ceases, and h_{conv} is the height of the convective zone where air mixing inhibits gravitational fractionation. If the h_{diff} is known then it is possible to calculate the $\delta^{15}N\text{-}N_2$ using the barometric equation (Sowers et al., 1992):

$$\delta^{15}N = \left[\left(e^{gh_{diff}/RT}\right) - 1\right] * 10^3 \qquad (2)$$

where g is the acceleration due to gravity (9.80 m/s^2), R is the gas constant (8.314 J mol^{-1} K^{-1}), and T is the ambient temperature (degrees Kelvin). We calculated the $\delta^{15}N$-N_2 expected at Taylor Glacier using $d_{close\text{-}off}$ = 30 m, h_{LIZ} = 3 m, and h_{conv} = 0 m (Figure S6). Introducing h_{conv} = 13.5 m is needed to bring the calculated $\delta^{15}N$-N_2 into agreement with the measured values presented in the main text (Figure S7). The height of the lock-in-zone (h_{LIZ} = 3 m) was estimated to be conservatively large, though note that this parameter does not significantly influence the $\delta^{15}N$-N_2 calculation. For example, reducing the lock in zone height by 50% only increases h_{diff} (and $\delta^{15}N$-N_2) by 5.5 %.

We repeated similar calculations for Taylor Dome at 60 ka. We used $d_{close\text{-}off}$ = 53 m, h_{LIZ} = 3 m, and h_{conv} = 0 m (Figure S8). We did not adjust h_{conv} to bring $\delta^{15}N$-N_2 into closer agreement with measured values because a target $\delta^{15}N$-N_2 value is ambiguous due to the lower resolution and precision of the data (see main text Figure 5d).

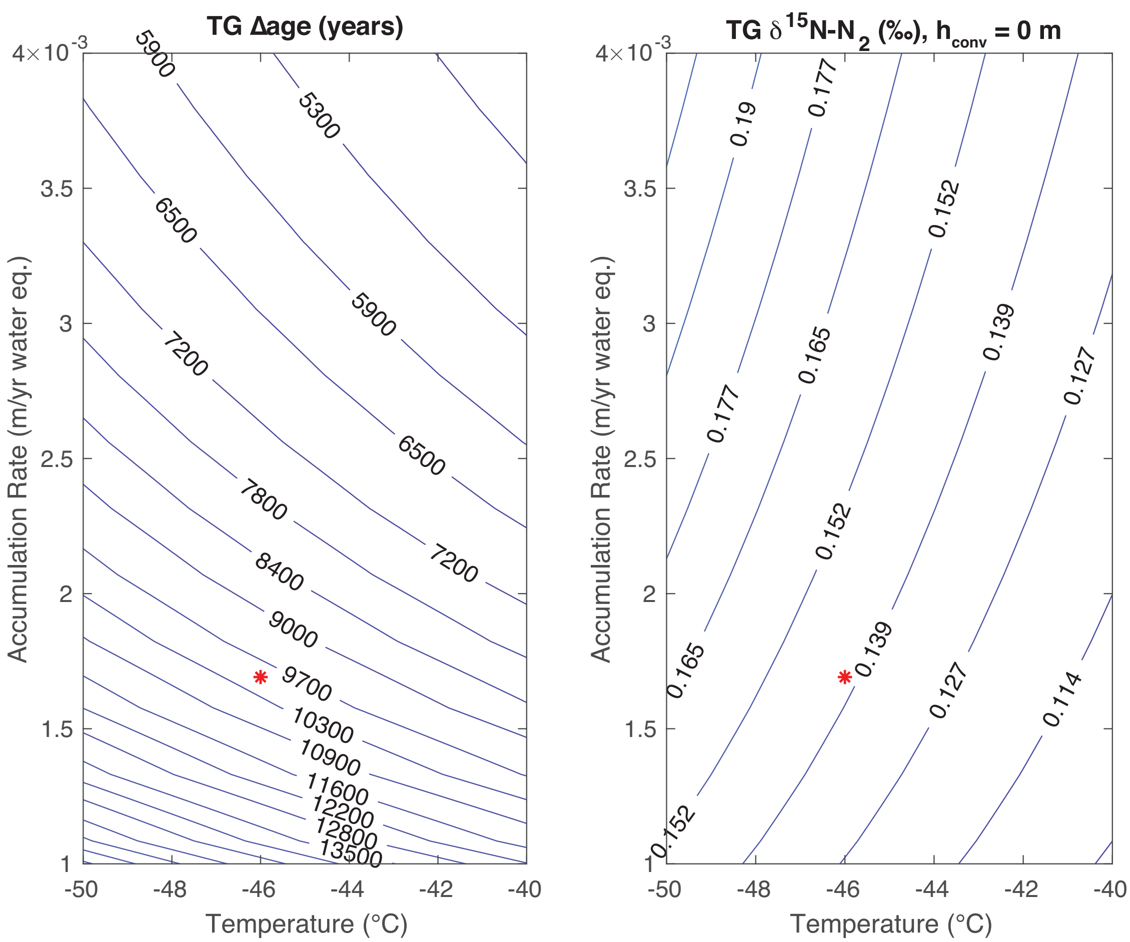

Figure S6 – Δage and $\delta^{15}N$-N_2 calculated using a firn densification model and the barometric equation for a range of accumulation rates and temperatures. It is possible to estimate the accumulation rate given independently determined Δage and temperature. The red star represents Taylor Glacier at 60 ka where Δage = 10,000 years (see main text).

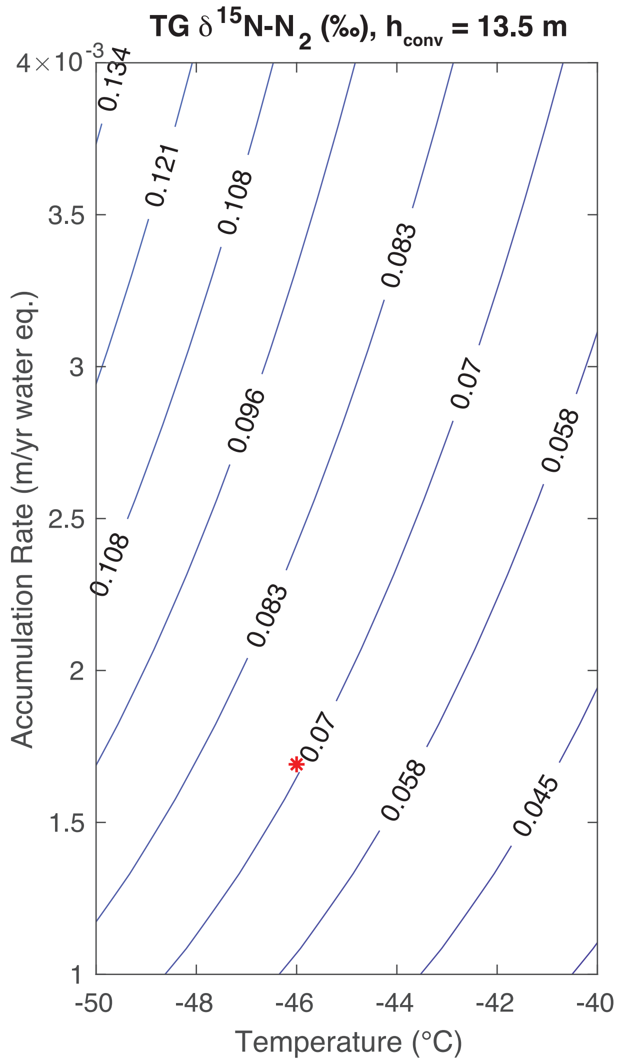

Figure S7 – δ^{15}N-N_2 calculated similarly to δ^{15}N-N_2 in Figure S6 but with h_{conv} = 13.5 m.

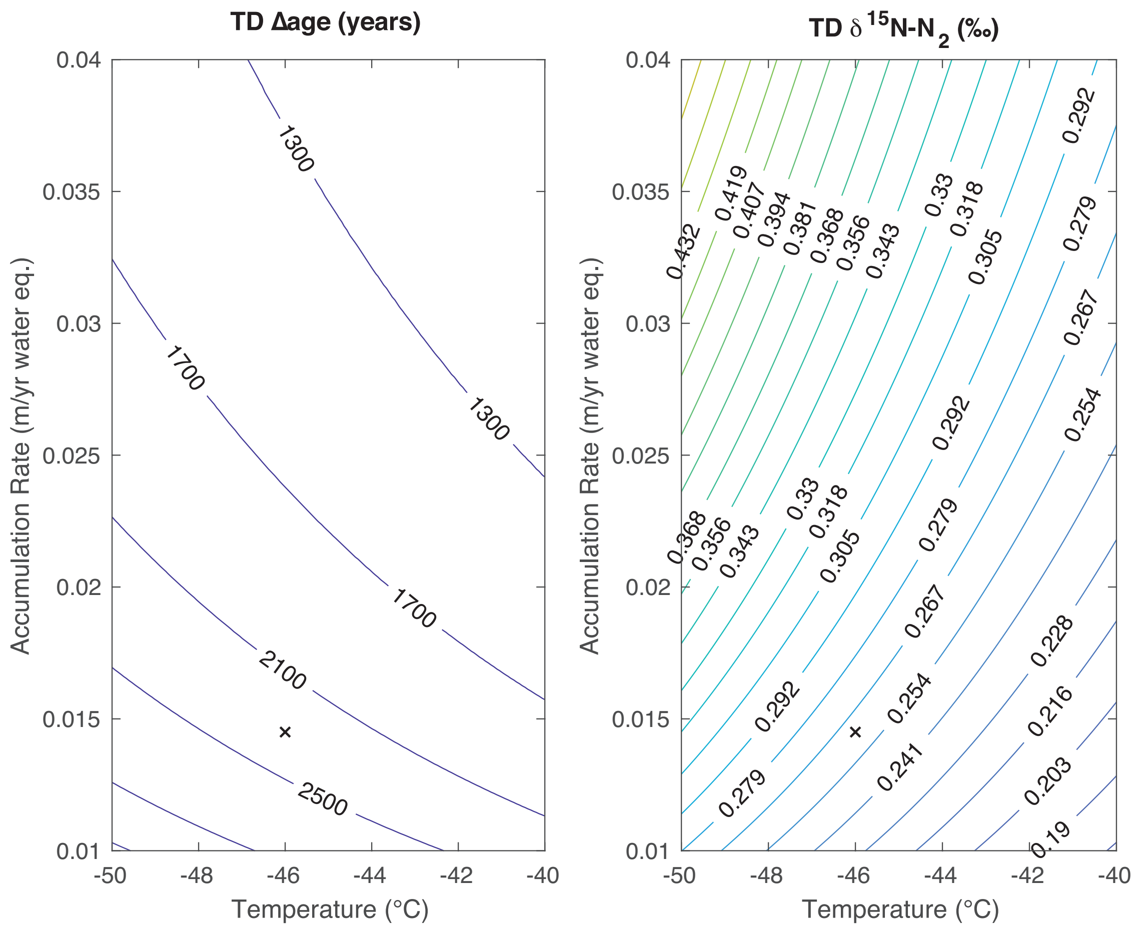

Figure S8 - Δage and $\delta^{15}N\text{-}N_2$ calculated using a firn densification model and the barometric equation for a range of accumulation rates and temperatures. The black x represents Taylor Dome at 60 ka where Δage = 2300 years.

References

Baggenstos, D., Severinghaus, J. P., Mulvaney, R., McConnell, J. R., Sigl, M., Maselli, O., Petit, J. R., Grente, B., and Steig, E. J.: A Horizontal Ice Core From Taylor Glacier, Its Implications for Antarctic Climate History, and an Improved Taylor Dome Ice Core Time Scale, Paleoceanogr. Paleoclimatology, 33, 778-794, 10.1029/2017pa003297, 2018.

Brook, E. J., Harder, S., Severinghaus, J., Steig, E. J., and Sucher, C. M.: On the origin and timing of rapid changes in atmospheric methane during the last glacial period, Global Biogeochemical Cycles, 14, 559-572, 10.1029/1999gb001182, 2000.

Capron, E., Landais, A., Lemieux-Dudon, B., Schilt, A., Masson-Delmotte, V., Buiron, D., Chappellaz, J., Dahl-Jensen, D., Johnsen, S., Leuenberger, M., Loulergue, L., and Oerter, H.: Synchronising EDML and NorthGRIP ice cores using delta O-18 of atmospheric oxygen (delta O-18(atm)) and CH4 measurements over MIS5 (80-123 kyr), Quat. Sci. Rev., 29, 222-234, 10.1016/j.quascirev.2009.07.014, 2010.

Herron, M. M., and Langway, C. C.: Firn densification - An empirical-model, Journal of Glaciology, 25, 373-385, 1980.

Jouzel, J., Masson-Delmotte, V., Cattani, O., Dreyfus, G., Falourd, S., Hoffmann, G., Minster, B., Nouet, J., Barnola, J. M., Chappellaz, J., Fischer, H., Gallet, J. C., Johnsen, S., Leuenberger, M., Loulergue, L., Luethi, D., Oerter, H., Parrenin, F., Raisbeck, G., Raynaud, D., Schilt, A., Schwander, J., Selmo, E., Souchez, R., Spahni, R., Stauffer, B., Steffensen, J. P., Stenni, B., Stocker, T. F., Tison, J. L., Werner, M., and Wolff, E. W.: Orbital and millennial Antarctic climate variability over the past 800,000 years, Science, 317, 793-796, 10.1126/science.1141038, 2007.

Lambert, F., Delmonte, B., Petit, J. R., Bigler, M., Kaufmann, P. R., Hutterli, M. A., Stocker, T. F., Ruth, U., Steffensen, J. P., and Maggi, V.: Dust-climate couplings over the past 800,000 years from the EPICA Dome C ice core, Nature, 452, 616-619, 10.1038/nature06763, 2008.

Lambert, F., Bigler, M., Steffensen, J. P., Hutterli, M., and Fischer, H.: Centennial mineral dust variability in high-resolution ice core data from Dome C, Antarctica, Climate of the Past, 8, 609-623, 10.5194/cp-8-609-2012, 2012.

Landais, A., Masson-Delmotte, V., Nebout, N. C., Jouzel, J., Blunier, T., Leuenberger, M., Dahl-Jensen, D., and Johnsen, S.: Millenial scale variations of the isotopic composition of atmospheric oxygen over Marine Isotopic Stage 4, Earth Planet. Sci. Lett., 258, 101-113, 10.1016/j.epsl.2007.03.027, 2007.

Mayewski, P. A., Twickler, M. S., Whitlow, S. I., Meeker, L. D., Yang, Q., Thomas, J., Kreutz, K., Grootes, P. M., Morse, D. L., Steig, E. J., Waddington, E. D., Saltzman, E. S., Whung, P. Y., and Taylor, K. C.: Climate change during the last deglaciation in Antarctica, Science, 272, 1636-1638, 10.1126/science.272.5268.1636, 1996.

Petit, J. R., Jouzel, J., Raynaud, D., Barkov, N. I., Barnola, J. M., Basile, I., Bender, M., Chappellaz, J., Davis, M., Delaygue, G., Delmotte, M., Kotlyakov, V. M., Legrand, M., Lipenkov, V. Y., Lorius, C., Pepin, L., Ritz, C., Saltzman, E., and Stievenard, M.: Climate and atmospheric history of the past 420,000 years from the Vostok ice core, Antarctica, Nature, 399, 429-436, 10.1038/20859, 1999.

Schilt, A., Baumgartner, M., Schwander, J., Buiron, D., Capron, E., Chappellaz, J., Loulergue, L., Schupbach, S., Spahni, R., Fischer, H., and Stocker, T. F.: Atmospheric nitrous oxide during the last 140,000 years, Earth Planet. Sci. Lett., 300, 33-43, 10.1016/j.epsl.2010.09.027, 2010.

Seltzer, A. M., Buizert, C., Baggenstos, D., Brook, E. J., Ahn, J., Yang, J. W., and Severinghaus, J. P.: Does delta O-18 of O-2 record meridional shifts in tropical rainfall?, Climate of the Past, 13, 1323-1338, 10.5194/cp-13-1323-2017, 2017.

Sowers, T., Bender, M., Raynaud, D., and Korotkevich, Y. S.: Delta-N-15 of N2 in air trapped in polar ice - A tracer of gas-transport in the firn and a possible constraint on ice age-gas age-differences, Journal of Geophysical Research-Atmospheres, 97, 15683-15697, 1992.

Steig, E. J., Brook, E. J., White, J. W. C., Sucher, C. M., Bender, M. L., Lehman, S. J., Morse, D. L., Waddington, E. D., and Clow, G. D.: Synchronous climate changes in Antarctica and the North Atlantic, Science, 282, 92-95, 10.1126/science.282.5386.92, 1998.

Wang, Y. J., Cheng, H., Edwards, R. L., An, Z. S., Wu, J. Y., Shen, C. C., and Dorale, J. A.: A high-resolution absolute-dated Late Pleistocene monsoon record from Hulu Cave, China, Science, 294, 2345-2348, 10.1126/science.1064618, 2001.